

Visual Servoing and Motion control of a robotic device in inspection and replacement tasks

Madhusmita Senapati, J.Srinivas, V.Balakrishnan

Abstract— This paper presents a generalized framework of an image-based visual servoing of an articulated arm which has to be deployed inside a simulated reactor vessel environment. Wall tiles of the vessel idealized as rectangular grids on a surface are to be inspected and an attempt is made to replace the damaged tiles during shutdown periods of the machine. The vision sensing methodology of the proposed arm is explained. The arm has a camera located at the wrist (eye-in-hand) and the control action has to be taken place at joint level. The preliminary results are only illustrated.

Index Terms—In vessel inspection, Kinematics, Manipulator deployment, Serial robot, Visual-servoing.

I. INTRODUCTION

In recent years, a wide variety of applications regarding autonomous robot behaviour in unknown environments have been developed. The new generation robots are adapted to changing conditions in real time. Such behaviour is necessary especially when facing difficult tasks in practice like search and rescue missions, reconnaissance, surveillance and inspection in complex and dangerous surroundings. As an example, remote handling robots used in inspection and maintenance of in-vessel components of fusion devices require a non-contact robust sensing system. In such instances, the robot vision is crucial, since it mimics human sense and allows for noncontact measurement from the environment. The control inputs for the robot motors are produced by processing image data (like extraction of contours, features, corners and other visual primitives). Basic purpose of visual control is to control the pose of the robot's end-effector relative to a target object or a set of target features. Visual servoing or visual servo control (VSC) involves various techniques from image processing, computer vision and control theory. Using such an approach, systems with low cost sensors and actuators can be developed. In VSC, the information from camera is used within the control loop to position the tracking device as per the requirement. The vision data may be acquired either from the camera that is placed directly onto the manipulator (eye-in hand) or at a fixed location in the scene (eye-to hand). The features on the image plane are servo-controlled to their goal positions. There are two traditional approaches among all the vision-based control schemes [1]: (i) position-based VSC and

(ii) image-based VSC. In position-based system, the control is performed in task-space based on the three-dimensional information retrieved from the image. Here, the camera pose is estimated using visual information and the control design is a classical state-space design. The quality of the response depends on the quality of the pose estimation and makes the control sensitive to camera calibration errors. In an image-based system, feedback is defined based on image-features and controller is designed to drive the image features towards a goal configuration. Thus, it implicitly solves the Cartesian motion planning problem. The approach is therefore, relatively robust to camera calibration and target modelling errors. Image-based approaches exploit basically 2D visual measurements such as points or lines tracked in the image during task execution.

Robot has several links and joints and each requiring a positioning reference in relation to the predefined origin point. The vision system defines image coordinates based on where the camera points-to without regard to a fixed reference origin. Pixel locations within an image frame must coincide with the corresponding robot coordinates in order for proper visual robotic guidance. Several works were reported in literature relating vision guided robotic systems. Early in 1985, Sanderson et al.[1] proposed an adaptive control approach for the nonlinear time-varying relationship between the robot pose and image features in image-based servoing. They described detailed simulations of image-based visual servoing for a variety of 3-degree of freedom manipulators. Seaden and Ang [2] worked-on relative target-object (rigid-body) pose estimation for vision-based control of industrial robots. They developed and implemented a closed-form target-pose estimation algorithm. Feddama [3] applied an explicit feature space trajectory generator and closed-loop joint control to overcome problems due to low visual sampling rate. Here, an experimental work based on image visual servoing of a 4-degree of freedom robot was presented. Hashimoto et al.[4] also illustrated simulations for comparing position-based and image-based approaches. Korayem et al.[5] designed and simulated vision-based control and performance tests for 3-P robot by visual C++ software. They used a camera which was installed on end-effector of the robot to find a target. A feature-based visual servoing control on the end-effector was used to reach the target. Jara et al.[6] employed Java for developing an interactive tool for industrial robot simulations. Pinto et al.[7] proposed a eye-on-hand system, where the use of cameras will be replaced by the 2D laser range finder, which is attached to a robotic manipulator executing predefined path to produce grayscale images of workstation. Fang et al.[8] proposed augmented reality in programming a robot for trajectory planning and transformation into task-optimized executable robot paths. Therefore, the impact of pose estimation in visual

Manuscript received April 20, 2014.

Ms.Madhusmitha Senapati, Department of Mechanical Engineering, National Institute of Technology, Rourkela, India, Ph:9040635247,

Dr.J.Srinivas, Department of Mechanical Engineering, National Institute of Technology, Rourkela, India, 769008, Ph.+91-661-2462503,

Dr.V.Balakrishnan, Institute of Plasma Research, Gandhinagar, India, Phone: +91-7923-962183,

servoing, where the relative pose between a camera and a target can be used for real-time control of robot motion is a topic of present interest.

In a fusion reactor, the first wall inside a shielded-blanket is a basic in-vessel component that often affected by the plasma strokes. In this regard, the tiles of first wall are supposed to withstand the intense flux of energetic particles (hydrogen isotopes and neutrons) as well as heat loads. It requires frequent inspection of wall tiles during shutdown periods. Remote in-vessel inspection and guided robotic systems are required in this regard. Several earlier works [9-13] have illustrated the implementation issues of robots in fusion reactor vessels with ITER standards. Designing such a robotic system involves multiple modules such as: flexible manipulator mechanism that advances freely into the ports of the vessel, gripper designing for handling the wall-tiles, vision-based inspection scheme for monitoring, as well as the remote control of joints as per the requirements. In the present work, vision module is presented for this specific application. The proposed 7-degrees of freedom articulated redundant robot manipulator configuration is first explained. Kinematics issues are briefly outlined. Vision sensing methodology in the proposed manipulator is described.

II. DESCRIPTION OF ROBOTIC MANIPULATOR

The manipulator considered in present wok is an articulated serial redundant platform. It can be controlled by a teach pendant or a joy-stick device. It has a sturdy base that can be moved on rails and locked at a particular position. Further, there is a waist which could be swivelled about vertical axis just like other industrial commercial arms. This is controlled by a high torque DC motor through metallic gear train. At the end of waist, there is a shoulder joint which is driven by another DC motor through belt-transmission. This link is further connected in succession with two more links as shown in Fig. 1.

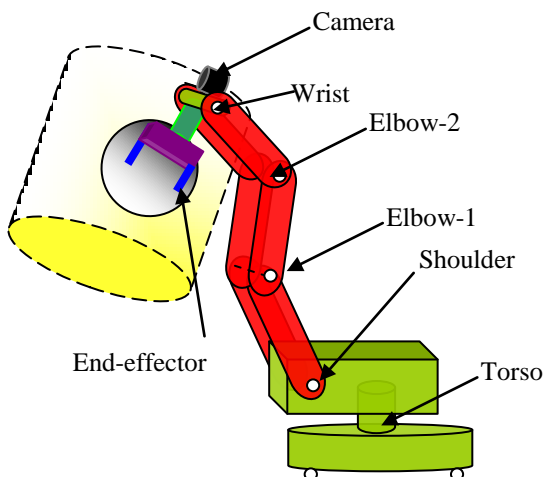


Fig.1 Schematic of the P6R manipulator system

The end of the final link is a place for joining with a wrist, which is controlled by joint motors facilitating the end-effector that holds a tool to advance to a required posture. In fact, the wrist pitch is controlled by a similar DC motor located at the base, while roll is guided by a relatively smaller

torque-rating motor mounted at the wrist. The end-effector is a two-state gripper with rubber pads and is operated by a worm-wheel based four bar mechanism. As the gripper will be activated after end-effector is aligned with target point, this translational degree of freedom is generally not considered in overall degrees of freedom of the manipulator. The visual sensor in this work is a digital camera mounted before the end-effector to monitor the target motion in a 3-dimensional (3D) workspace. The camera is assumed calibrated and the intrinsic and extrinsic parameters, such as the focal length, the physical size and resolution of image sensor, the transformation matrix between the camera and the end-effector, are known.

A. Kinematic Model

Kinematic model refers to the methodology of deriving the relationship between joint angles and the end-effector pose. Conventional Denavit- Hartenberg (D-H) notation of link frames is adopted and parameters are first identified. The link homogeneous transformation matrices are first obtained from the table of known and unknown variables. Fig. 2 shows the kinematic link frames considered for further analysis.

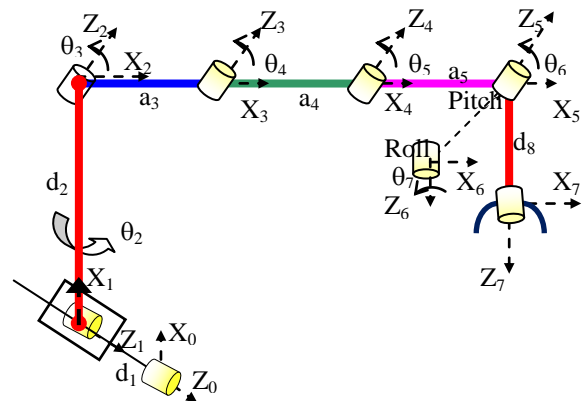


Fig. 2 Kinematic model of the manipulator

The D-H parameters of the manipulator are shown in Table-I.

TABLE I
D-H PARAMETERS OF THE MANIPULATOR

Link	θ	d	a	α	Joint limits
1	0	d_1	0	0	0-800 mm
2	θ_2	d_2	0	$-\pi/2$	-170° to 170°
3	θ_3	0	a_3	0	-60° to 90°
4	θ_4	0	a_4	0	-45° to 70°
5	θ_5	0	a_5	0	-45° to 70°
6	θ_6	0	0	$-\pi/2$	-170° to 170°
7	θ_7	0	0	0	-100° to 100°

The transformation matrix of the coordinate system (frame) i , represented in frame $i-1$ can be written as:

$${}_{i-1}T_i = \begin{bmatrix} c\theta_i & -s\theta_i c\alpha_i & s\theta_i s\alpha_i & a_i c\theta_i \\ s\theta_i & c\theta_i c\alpha_i & -c\theta_i s\alpha_i & a_i s\theta_i \\ 0 & -s\alpha_i & c\alpha_i & d_i \\ 0 & 0 & 0 & 1 \end{bmatrix}, (i=1,2,\dots,7) \quad (1)$$

where, θ_i , d_i , a_i , α_i are the D-H parameters of link i as shown in Table I, with $c=\cos$ and $s=\sin$. The link lengths $a_3=a_4=a_5=240\text{mm}$ and waist height $d_1=300\text{mm}$, The overall

forward kinematics ${}^0T_7 = {}^0T_1[{}^1T_2][{}^2T_3] \dots [{}^6T_7]$ of the manipulator can be easily obtained by multiplying individual link transformation matrices. This can be done with symbolic programming available in MATLAB/Maple environment. In control task, the joint motors are actuated as per the sensing information available from Cartesian space. Inverse kinematics therefore, computes the required joint angles when the pose of the end-effector is supplied (see appendix). The Jacobian matrix describing the relationship between the joint angular velocities and the corresponding end-effector linear velocities can be then obtained with the method of differential transformations.

B. Frames of Reference

It is assumed that a camera is rigidly mounted over the wrist and that the object is placed in the camera's field of view as shown in Fig.3.

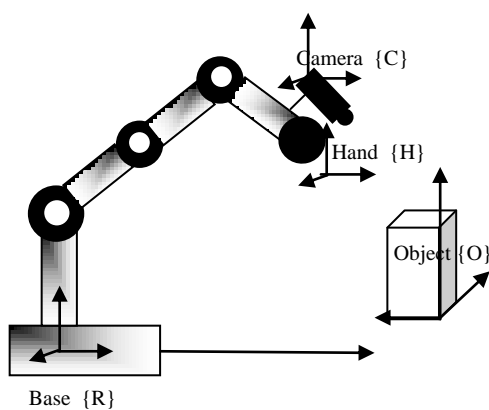


Fig.3 Frames of Reference

The relevant four coordinate frames are: the object frame $\{O\}$ centered at the object, the camera frame $\{C\}$ centered at the camera lens, the manipulator hand frame $\{H\}$ centered at the robot end-effector and the robot base frame $\{R\}$ centered at the robot base. In practice, locating an object with respect to the robot base requires: (i) camera calibration, which describes the relative position and orientation between the object and the camera C_OT (ii) hand-eye calibration, which describes the relative position and orientation between the camera and the robot hand ${}^H_C T$ and (iii) robot calibration, which is the manipulator kinematics relating hand frame with respect to base ${}^R_H T$. Given a point P on the object (in homogeneous coordinates), the point described in the robot frame is given by

$$\{^R P\} = [{}^R_OT] \{^O P\} \quad (2)$$

where

$$[{}^R_OT] = [{}^C_OT][{}^H_C T][{}^R_H T] \quad (3)$$

is a 4×4 homogeneous Euclidean transformation between the object and robot coordinate frames.

III. INTRODUCTION TO IMAGE-BASED VISUAL SERVOING

A visual servoing task is in fact minimization of an error vector defined in image plane. When a number of image features on the image plane are given, it is required to select a

set of generalized image coordinates to characterize them. Let $s(q(t), \lambda)$ be the generalized image coordinates with λ representing the geometric parameters associated with the features in the 3-D space. Then, the error vector is defined as:

$$e(t) = s(q(t), \lambda) - s^* \quad (4)$$

Here, s^* is the desired feature information vector. The definition of parameter vector 's' determines the visual servo control scheme. To design visual servo controller, a relationship between the time derivative of s and camera velocity v_c is first determined as follows:

$$\dot{s} = L_s v_c \quad (5)$$

Where, L_s is called image Jacobian matrix. Now, the relationship between the camera velocity and error vector is obtained by considering s^* to be constant parameter (due to fixed goal pose) as follows:

$$\dot{e} = L_s v_c \quad (6)$$

In order to decrease the error, $\dot{e} = -\lambda e$ is chosen, resulting in

$$v_c = -\lambda L_s^+ e \quad (7)$$

Here, L_s^+ is pseudo inverse matrix of L_s , which cannot be calculated in real conditions and hence an approximation \hat{L}_s^+ is often used. Fig.4 shows a relationship between the camera frame and the image frame.

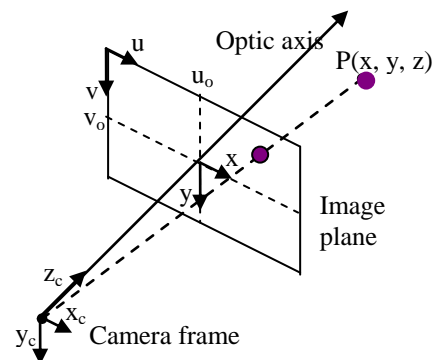


Fig.4 Image and camera frames

A 3D point P can be projected into the image plane as a 2D point using the perspective projections as:

$$x = \frac{X}{Z} = \frac{u - u_0}{f} \quad (8)$$

$$y = \frac{Y}{Z} = \frac{v - v_0}{f} \quad (9)$$

The parameters u_0, v_0, f are called the camera intrinsic parameters. The velocity of 3D point referring to camera frame is:

$$\dot{P} = -\dot{v}_c - \omega_c \times P \quad (10)$$

Where v_c and ω_c is instantaneous linear and angular velocities of camera. Here, $P = [x \ y \ z]^T$ is a point on 3D object. Using eqs.(8) and (9) along with eq.(10), we can simplify and write down the relations as:

$$\dot{X} = L_x V_c \quad (11)$$

Where $X = [x \ y]^T$ and $V_c = [v_x \ v_y \ v_z \ \omega_x \ \omega_y \ \omega_z]^T$ are vectors. The matrix L_x is image Jacobian given by [14]:

$$\mathbf{L}_x = \begin{bmatrix} -\frac{1}{Z} & 0 & -\frac{x}{Z} & xy & -(1+x^2) & y \\ 0 & -\frac{1}{Z} & -\frac{y}{Z} & (1+y^2) & -xy & -x \end{bmatrix} \quad (12)$$

Here, the depth Z should be accurately measured; otherwise an estimate \hat{L}_x should be used.

IV. PROPOSED METHODOLOGY

The control problem can be defined as follows: Design a set of joint trajectories, such that the end-effector can move to a desired grasp position using the available pose of target in the workspace obtained from vision system. Fig.5 shows the workspace of the manipulator. The assembly of articulated robotic manipulator is tested in CATIA and the parts are exported to ADAMS VIEW (R2013). The various joints are applied to visualize the kinematic simulations.

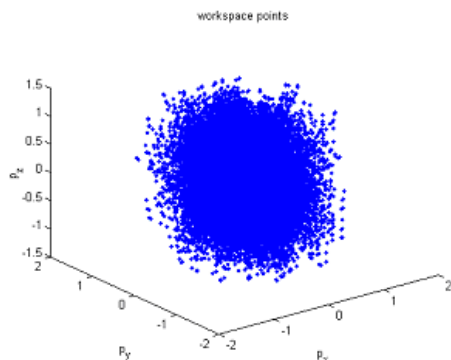


Fig.5 Work volume at the end-effector

Various steps involved in the process of vision-based monitoring are: (i) digital image acquisition (ii) pre-processing (filtering etc) (iii) feature extraction (to acquire import image features like lines, edges) (iv) detection/segmentation (to determine image points or regions for further processing) and (v) decision making. The automated tile-inspection procedure is explained below: (a) to capture the image, a digital camera (BASLER acA640-90gm) with the Sony ICX424 CCD sensor delivering 90 frames per second at 1.4 MP resolution is employed. It has 659 (Horizontal) x 494 (vertical) pixels. Fig.6 shows the camera used. It can be interfaced with PC using Ethernet port and operates with a 12 V DC power supply. It is to be mounted at the end of arm and care has to be taken to reduce image blurring.



Fig.6 Digital camera employed

Image processing techniques like median filtering, contrasting, brightness and edge sharpening have to be applied to enhance the quality of interested points and to

remove the noise. There are basically two kinds of image enhancement techniques: spatial domain methods and frequency-domain methods. Spatial domain methods directly deal with image pixels. The pixel values are manipulated to achieve desired enhancement of image. In frequency domain methods, the image is first transferred into frequency domain (i.e., Fourier transform of the image is first computed). Then all enhancement operations are performed and finally inverse Fourier transforms is performed to get the resultant image.

In typical visual inspection of tiles of the reactor vessel, a sector of the entire surface is scanned from left to right in top-bottom direction. For simulation sake, tiles are represented with rectangular grids drawn on a paper and the paper is affixed to a cylindrical tank as shown in Fig.7.



Fig.7 Simulated set-up of vessel tile

Some of the grids are having a point (crack) or vertical line (crack) or inclined line (cracks) etc. as shown in Fig.8. The task is to predict the nature of the crack first using visual image processing.

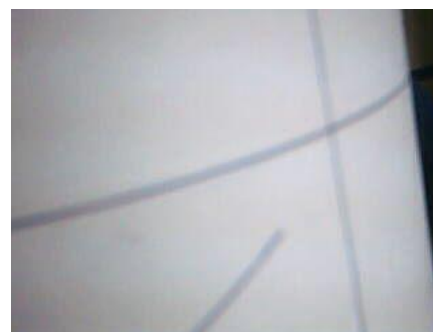


Fig.8 Tile having inclined crack

The image processing operation is planned through LabVIEW software as shown in Fig.9.

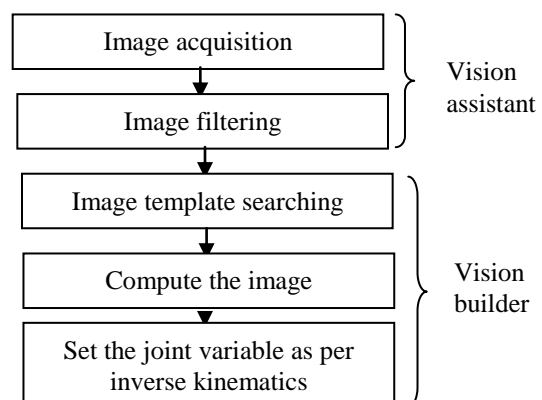


Fig.9 Real time maintenance

V. CONCLUSION

In this paper, some outlines of the image-based vision servoing approach with a redundant 7-DOF manipulator possessing eye-in-hand configuration have been briefed-out. The kinematics of the manipulator, vision system employed were explained. The simulated environment of wall tiles of reactor vessel was described. As a future scope the camera has to be attached to the end of arm and the captured images are to be processed for prediction of type of fault and the gripper tactile sensing issues as well the faulty tile removal matters will be considered.

APPENDIX

Derivation of inverse kinematics of the present manipulator is based on the derivation of the inverse kinematics of a PUMA 560 robot. Rotation of first rotational axis θ_2 is obtained by writing in following form:

$${}^0_2T^{-1}{}^0_7T = {}^2_3T{}^3_4T{}^4_5T{}^5_6T{}^6_7T = {}^0_2T^{-1} [T] \quad (A1)$$

where, [T] is the actual orientation and position of end-effector given by:

$$[T] = \begin{bmatrix} n_x & o_x & a_x & p_x \\ n_x & o_x & a_y & p_y \\ n_x & o_x & a_z & p_z \\ 0 & 0 & 0 & 1 \end{bmatrix} \quad (A2)$$

Equating the (2,4) elements on both sides of eq.(A1), we get

$$-s_2p_x + c_2(d_1 - p_z) = 0 \quad (A3)$$

which gives

$$\theta_2 = \text{atan2}(d_1 - p_x, p_z) \quad (A4)$$

$$\theta_2 = \pi + \text{atan2}(d_1 - p_x, p_z) \quad (A5)$$

When θ_2 is known the transform ${}^0_2T(d_1, \theta_2)$ is fully defined. Rotation θ_4 is obtained by equating elements (1,4) and (3,4) on both sides of eq.(A1):

$$c_2p_x + s_2(d_1 - p_z) = a_4c_3c_4 + a_5s_3s_4 + a_4c_3 + a_3 \quad (A6)$$

$$p_y - d_2 = -a_5s_3c_4 - a_5c_3s_4 - a_4c_3 \quad (A7)$$

These equations give two sets of θ_4 . The rotation θ_3 can be obtained by writing

$${}^0_4T^{-1}{}^0_7T = {}^4_5T{}^5_6T{}^6_7T \quad (A8)$$

Equating elements (1,4) and (3,4) from both sides of eq.(A8), we get an expression of the form:

$$\theta_3 + \theta_4 = \text{atan2}(K_1, K_2) \quad (A9)$$

Since 4 combination of solutions of θ_2 and θ_4 exists, θ_3 will have 4 possible solutions. The process is continued for θ_5 . Finally, a given wrist position can be achieved by 4 combinations of the 4 joint rotations $\theta_2, \theta_3, \theta_4$ and θ_5 . The pitch and roll angles of the wrist θ_6 and θ_7 are obtained by equating the terms in rotational matrices.

ACKNOWLEDGMENT

Authors thank the board of research in fusion science and technology (BRFST) for sponsoring and financial support in this project.

REFERENCES

- [1] A.C.Sanderson, L.E.Weiss, and C.P. Neuman, "Dynamic Visual servo control of robots: an adaptive image-based approach", Proc. *IEEE Robotics and Automation*, Pittsburgh, 1985, Vol.2, pp.662-667.
- [2] M.Saedan and M.H.Ang, "3D Vision-based control of an industrial robot", Proc. *Iasted Int. Conf. Robotics and Applications*, Nov.19-22, 2001, Florida, Kpp.152-157.
- [3] J.T.Feddema, C.S.G. Lee and O.R.Mitchell, "Weighted selection of image features for resolved rate visual feedback control", *IEEE Trans. Robotics and Autonomous Systems*, Vol.7, 1991, pp.31-47.
- [4] H.Hashimoto, T.Kimoto and T.Ebin, "Manipulator control with image-based visual servoing", Proc.IEEE Conf. *Robotics and Automation*, 1991, pp.2267-2272.
- [5] M.H.Korayem, K.Khoshhal and A.Aliakbarpour, "Vision-based robot simulation and experiment for performance tests of robot", *Int .J. Adv. Manuf. Tech.*, Vol.25, 2005, pp.1218-1231.
- [6] C.A.Jara, F.A.,Candek, P.Gil, F. Torres, F. Esquemre and S.Dormido, "EJS+EJSRL: An interactive tool for industrial robot simulation, computer vision and remote operation", *Robotics and Autonomous systems*, Vol.59, 2011, pp.389-401.
- [7] A.M.Pinto, L.F.Rocha and A.P..Moreira, "Object-recognition using laser-range finder and machine learning techniques", *Robotics and Computer-Integrated Manufacturing*, Vol.29, 2013, pp.12-22.
- [8] H.C.Fang, S.K.Ong, and A.Y.C.Nee, "Interactive robot trajectory planning and simulation using augmented reality", *Robotics and Computer-Integrated Manufacturing*, Vol.28, 2012, pp.227-237.
- [9] L.Gargiulo, P.Bayetti, V.Bruno, J.J.Cordier, "Development of an ITER relevant inspection robot", *Fusion Engg., and Design*, vol.83, 2008, pp.1833-1836.
- [10] A.Mutka, I.Draganac, Z.Kovacic, Z.Postruzin and R.Munk, "Control system fro reactor vessel inspection manipulator", 18th IEEE Int. Conf. Control Application, St Petersburg, Russia, 2009, p.1312.
- [11] J.M.Traverse, "In-vessel component imaging systems: From the present experience towards ITER safe operation", *Fusion Engineering and Design*, vol.84, pp.1862-1866, 2009.
- [12] M.Hourly, P.Bayetti, D.Keller, L.Gargiulo, V.Bruno and J.C.Hatchressaian, "Development of in-situ diagnostics and tools handled by a light multipurpose carried for tokamak in-vessel interventions", *Fusion Engineering and Design*, vol.85, 2010, p.1947.
- [13] X.Peng, J.Yuan, W.Zhang, Y.Yang, Y.Song, 'Kinematic and dynamic analysis of a serial robot for inspection process in EAST vacuum vessel", *Fusion Engg., and Design*, vol.87, 2012, pp.905-909.
- [14] B.P.Larouchi and Z.H.Zhu, 2014, Autonomous robotic capture of non-cooperative target using visual servoing and motion predictive control , *Auton Robot*, DOI 10.1007/s10514-014-9383-2.

Madhusmitha Senapati is pursuing M.Tech Research in the area of Robotics and Vision-based inspection at NIT Rourkela. She graduated in Mechanical Engineering discipline from Utkal University. .

Dr.J.Srinivas is an Associate Professor in department of Mechanical Engineering, NIT Rourkela. His topics of interest include: robotics and intelligent controls, dynamics and modeling. He guided various graduate and doctoral projects. He is a member of Institute of Engineers and has to his credit around 80 papers published in various national and international conferences/journals. He is a main author of a book on Robotics: Control and Programming published by Narosa Publishing house. .

Dr.V.Balakrishnan is a senior scientist at institute of plasma research, Gandhinagar and is presently working for indigenous tokamak vessel Aditya. He has good expertise with earlier vessels 'SSR-I' and 'SSR-II'.